Quantitative Analysis of Endocardial and Epicardial Left Ventricular Myocardial Deformation in Patients with Cardiac Amyloidosis

Ayako KOZUKA[1)3)*], Jun KOYAMA[1)4)], Yoshiki SEKIJIMA[2)] and Uichi IKEDA[1)5)]

1) *Department of Cardiovascular Medicine, Shinshu University School of Medicine*
2) *Department of Medicine (Neurology and Rheumatology), Shinshu University School of Medicine*
3) *Minaminagano Medical Center Shinonoi General Hospital*
4) *Internal Medicine, Maruko Central Hospital*
5) *Nagano Municipal Hospital*

Background : Studies using cardiovascular magnetic resonance imaging have demonstrated subendocardial deposition of amyloid protein in patients with cardiac amyloidosis (CA). We examined whether subendocardial dysfunction due to amyloid deposition exists in patients with CA.

Methods : We examined 98 consecutive patients with CA and 20 control individuals. CA patients were divided into three groups. Group 1 had no evidence of cardiac involvement (n = 32), group 2 had heart involvement but no congestive heart failure (CHF) and/or serum brain natriuretic peptide (BNP) levels < 100 pg/mL (n = 23), and group 3 had heart involvement and CHF and/or serum BNP levels ≥ 100 pg/mL (n = 43). Circumferential, radial, and longitudinal strains of the inner half and outer half layers of the left ventricular (LV) wall were examined.

Results : There was no significant difference in strain parameters between those with AL and ATTRm amyloidosis. There were no significant differences in circumferential inner/outer strain among the 4 groups. Regarding radial strain, groups 2 and 3 had a depressed inner radial strain compared with group 1 in the entire basal and mid-LV wall ($P < 0.001$, one-way analysis of variance) and that in group 1 was smaller than that in controls. Longitudinal strains of the inner/outer layers in the basal and mid-LV wall were significantly depressed with apical sparing in groups 2 and 3 compared with those in group 1.

Conclusions : In patients with CA, complete endomyocardial radial systolic dysfunction and longitudinal transmural systolic dysfunction exist in the basal and mid-LV wall. *Shinshu Med J 67 : 49—62, 2019*

(Received for publication August 17, 2018 ; accepted in revised form October 11, 2018)

Key words : subendocardial dysfunction, cardiac amyloidosis, speckle tracking echocardiography

Abbreviations : 2D = 2-dimensional, A = peak velocities of late-filling wave, AL = light-chain associated, ATTRm = mutated transthyretin associated, CA = cardiac amyloidosis, CHF = congestive heart failure, CMRI = cardiovascular magnetic resonance imaging, D = diastolic, E = peak velocities of early diastolic wave, e' = early diastolic mitral annular velocities, LA = left atrium, LV = left ventricular, ROI = region of interest, S = systolic, SD = standard deviation, TTR = tansthyretin

I Introduction

Cardiac amyloidosis (CA) is a cardiomyopathy due to interstitial myocardial infiltration of amyloid, which leads to a progressive increase of ventricular wall thickness and stiffness[1)-5)].

CA is morphologically characterized by increased left ventricular (LV) wall thickness, normal or decreased LV cavity size, and congestive heart failure (CHF) with normal or near-normal fractional shortening[6)-10)]. Doppler flow parameters, tissue Doppler, and speckle tracking echocardiography can detect characteristic myocardial abnormalities, and several

* Corresponding author : Ayako Kozuka
Department of Cardiovascular Medicine,
Shinshu University School of Medicine, 3-1-1
Asahi, Matsumoto, Nagano 390-8621, Japan
E-mail : aya530705@yahoo.co.jp

parameters had been proven as prognosticators in patients with CA[11)-21)].

Recent studies using cardiovascular magnetic resonance imaging (CMRI) have demonstrated subendocardial deposition of amyloid protein in patients with CA[22)-24)].

A multi-layer approach of measuring myocardial strain can be performed using a commercially available echocardiographic machine[25)]. Thus, we hypothesized that complete subendocardial dysfunction due to subendocardial dominant amyloid deposition may exist in patients with CA. We therefore performed this study to quantify myocardial deformation of the inner half and outer half layers of the left ventricular wall (LV) using a multi-layer approach of measuring myocardial strain by 2-dimensional (2D) speckle tracking echocardiography.

Ⅱ Methods

A Study population

This study was approved by the Ethics Committee of Shinshu University School of Medicine, and written informed consent was obtained from each patient. Ninety-eight patients with systemic amyloidosis and 20 control individuals were enrolled in this study. A diagnosis of amyloidosis was made by a biopsy of involved organs, which demonstrated the typical Congo-red birefringence when viewed under polarized light. All patients were examined by myocardial ^{99m}Tc pyrophosphate scintigraphy. ATTRm amyloidosis was diagnosed from amyloid deposition in the abdominal fat pad (n＝35), endocardium (n＝4), stomach (n＝5), duodenum (n＝5), colon (n＝2), skin (n＝2), and sural nerve (n＝7), and from a biopsy of the carpal tunnel (n＝1); some patients had several biopsy specimens. The TTR mutations were as follows: (i) V30M (n＝43), (ii) D38A (n＝2), (iii) E54K (n＝2), (iv) E42G (n＝1), (v) I107V (n＝1), (vi) S50I (n＝1), (vii) S50R (n＝1). AL amyloidosis was confirmed by the findings of a monoclonal protein in the serum or urine and/or a monoclonal population of plasma cells in the bone marrow when evaluated by immunohistochemistry. For ATTRm amyloidosis, TTR gene analysis was routinely performed, as previously described[26)27)]. Forty-seven patients had AL amyloidosis, and 51 had ATTRm amyloidosis. Plasma levels of the brain natriuretic peptide (BNP) were measured on the day of echocardiography. Sixty-six patients met the echocardiographic criteria for cardiac involvement, and 32 had no apparent features of CA. The latter group was defined as group 1 (noncardiac amyloid) as we described previously[15)16)]. Definite cardiac involvement was defined as a mean echocardiographic end-diastolic LV wall thickness＞12 mm (half the sum of the thicknesses of the ventricular septum and posterior wall) in the absence of hypertension, valvular heart disease, diabetes mellitus, or criteria for LV hypertrophy on the electrocardiogram. Some patients with ATTRm amyloidosis had gait impairment due to peripheral nerve neuropathy, which limits behavior and masks CHF symptoms. In such patients, plasma BNP levels≥100 pg/mL were used as the criterion for CHF. Of 66 patients with cardiac involvement, 43 had prior or current evidence of CHF or plasma BNP levels≥100 pg/mL. These patients were defined as group 3 (CHF[＋]) and the remaining 23 patients were defined as group 2 (CHF[－]).

B Ultrasound examination and measurements

Echocardiographic examinations were performed using an ultrasound system with an S5-1 transducer (IE-33, Philips, Andover, Massachusetts). All imaging data for three cardiac cycles were digitized and stored on a disk for offline analysis. Parasternal and apical projections were obtained according to the recommendations of the American Society of Echocardiography[28)29)]. Standard M-mode measurements of the left atrium (LA) and LV wall were made. Pulsed Doppler echocardiography was used to obtain the transmitral and pulmonary venous flow velocities. Early diastolic mitral annular velocities of the septal and lateral mitral annulus (e') were obtained by pulsed tissue Doppler imaging. Peak velocities of early- (E) and late filling (A) waves, the duration of A-wave, the E/A ratio, and deceleration time of the E-wave were measured from transmitral flow velocities, and the peak velocities of the systolic (S), diastolic (D), and A waves; duration of A-wave; and D/

S ratio were measured from pulmonary venous flow. The E/e' ratio was also calculated.

C Myocardial strain measurements

Speckle tracking echocardiographic analysis for myocardial strain measurements was performed on LV short-axis images at the basal and mid-ventricular levels and on apical 2- and 4-chamber, and long-axis chamber views using speckle tracking echocardiographic software (QLAB, version 8.1, Philips). Circumferential, radial, and longitudinal strains of the inner half and outer half layers of the LV wall were semi-automatically calculated. Following initialization, the computer automatically formed a region of interest (ROI). An 18-segmental LV model was preset in the speckle tracking modality with six evenly divided segments in each of the short-axis views at the basal and mid-LV levels. Segmental circumferential, radial, and longitudinal strains were measured in all the short-axis views and in all three longitudinal views. In each segment, both the subendocardial and subepicardial circumferential, radial, and longitudinal strains were measured. Furthermore, mean values of the subendocardial and subepicardial myocardial layers were calculated as global circumferential, radial, and longitudinal strains.

The second set of measurements was performed two weeks after the first set of measurements for both inter- and intraobserver variability. Results are expressed as the linear regression between two measurements and as the percent error.

D Statistical analysis

All data were then expressed as mean ± standard deviation (SD). Statistical analyses were performed using a commercially available software program (JMP9.0.2, SAS Institute, Cary, North Carolina and Graph Pad Prism 5 for Mac OS X, Graph Pad, San Diego, California). Differences among characteristics of the three groups were assessed using the chi-square test for categorical variables, and comparisons of continuous variables among three groups were made using 1-way analysis of variance with Tukey-Kramer's HSD test for parametric variables, and the Kruskal-Wallis test with Dunn's post-hoc test for nonparametric variables. Bland-Altman analysis was conducted to assess intra- and interobserver agreements (expressed as the absolute value of mean difference ± 1.96 SD), and intraclass correlation coefficients were calculated. A difference was considered significant when the P value was < 0.05.

Ⅲ Results

A Qualitative myocardial ^{99m}Tc pyrophosphate scintigraphy

Fifty of 51 patients with ATTRm showed a positive shadow on myocardial ^{99m}Tc pyrophosphate scintigraphy, and all patients with AL showed negative myocardial accumulation.

B Patients' characteristics and 2D echocardiography

Patients' clinical characteristics are shown in **Table 1**. Patients' age was greater in group 3 than in group 1. The diastolic blood pressure was significantly lower in group 3 than in the other two groups. Plasma BNP levels were greater in group 3 than in group 1. The LA diameter was significantly greater in groups 2 and 3 than in group 1. The predefined LV wall thickness was larger in groups 2 and 3 than in group 1. The LV ejection fraction was significantly smaller in group 3 than in the normal group and group 2.

C Standard doppler flow and tissue doppler measurements

Indexes of transmitral flow, pulmonary venous flow, systolic/diastolic time intervals, and tissue Doppler in the mitral annulus are shown in **Table 2**. Group 3 had more abnormalities in Doppler flow velocity pattern, and E/e' than in the other 3 groups.

D Global and segmental LV strain values

Global circumferential, radial, and longitudinal strain values of the inner and outer myocardial layers are shown in **Table 3**. There were no significant differences in global circumferential strain of the inner and outer myocardium layers among three groups. Basal global radial strain was smaller in groups 2 and 3 than in group 1 for both the inner and outer layers. Furthermore, inner global radial strain was significantly smaller in group 1 than in controls. In the mid-LV wall, global inner radial strain was smaller in groups 2 and 3 than in group 1,

Table 1　Patients' characteristics and 2-dimensional Echo-parameters (Mean ± SD)

Variable	Normal	Group 1 (No LVH)				Group 2 (LVH)				Group 3 (CHF)			
	(n = 20)	Overall (n = 32)	AL (n = 22)	ATTRm (n = 10)	P value	Overall (n = 23)	AL (n = 9)	ATTRm (n = 14)	P value	Overall (n = 42)	AL (n = 16)	ATTRm (n = 27)	P value
Age (years)	56 ± 14	56 ± 13	61 ± 6	45 ± 16	0.002	60 ± 11	60 ± 10	61 ± 11	0.850	64 ± 12‡‡	61 ± 11	66 ± 11	0.092
Male/female	10/10	15/17	11/11	4/6	0.59	18/5	7/2	11/3	0.964	26/17	10/6	16/11	0.833
HR (beats/min)	63 ± 10	65 ± 8	63 ± 7	70 ± 6	0.025	67 ± 16	73 ± 20	63 ± 11	0.207	67 ± 13	78 ± 13	61 ± 9	0.0001
SBP (mmHg)	115 ± 12	116 ± 16	116 ± 15	116 ± 18	0.84	122 ± 23	118 ± 24	124 ± 22	0.571	110 ± 20	107 ± 17	113 ± 21	0.422
DBP (mmHg)	75 ± 11	76 ± 12	78 ± 13	73 ± 12	0.393	79 ± 16	79 ± 17	79 ± 16	0.950	68 ± 12‡‡ §§	70 ± 13	67 ± 11	0.697
BNP (pg/mL)	-	22 ± 19	19 ± 15	28 ± 27	0.60	57 ± 57	100 ± 113	49 ± 21	0.40	409 ± 903§§	662 ± 1453	254 ± 185	0.12
LAD (mm)	36.5 ± 6.0	33.8 ± 5.0	34.4 ± 5.3	32.5 ± 4.4	0.416	37.8 ± 7.0‡	36.5 ± 4.7	38.6 ± 8.2	0.219	41.1 ± 6.7†	42.0 ± 7.7	40.5 ± 6.2	0.386
LV EDD (mm)	45.9 ± 5.2	44.6 ± 4.5	45.5 ± 4.9	42.5 ± 2.2	0.025	41.9 ± 4.7	41.6 ± 6.5	42.1 ± 3.2	0.850	41.7 ± 5.8	40.6 ± 6.7	42.4 ± 5.2	0.555
LV ESD (mm)	27.3 ± 4.0	25.7 ± 3.7	26.4 ± 4.0	24.2 ± 2.6	0.080	24.9 ± 4.5	23.5 ± 4.3	25.8 ± 4.5	0.328	25.8 ± 5.5	25.1 ± 6.4	26.2 ± 4.9	0.688
LVFS (%)	40.2 ± 5.3	42.4 ± 5.2	42.1 ± 5.7	43.1 ± 4.0	0.416	40.8 ± 7.3	43.7 ± 4.3	39.0 ± 8.3	0.083	38.3 ± 10.4	38.5 ± 13.3	38.1 ± 8.5	0.910
IVSThd (mm)	10.0 ± 1.1	9.9 ± 1.6	9.6 ± 1.6	10.5 ± 1.6	0.173	15.5 ± 3.1*†	15.4 ± 1.7	15.7 ± 3.7	0.728	17.3 ± 5.0*†	16.2 ± 3.5	18.0 ± 5.6	0.218
LVPWThd (mm)	9.9 ± 0.8	8.9 ± 1.5	8.9 ± 1.6	8.9 ± 1.3	0.887	13.4 ± 2.6*‡‡	13.2 ± 2.4	13.5 ± 2.8	0.975	14.8 ± 3.8*†	14.8 ± 3.8	14.7 ± 3.9	0.99
LVEF (%)	64.1 ± 4.0	61.0 ± 5.7	60.4 ± 6.3	62.4 ± 4.0	0.356	63.5 ± 5.9	61.8 ± 5.3	64.6 ± 6.3	0.269	58.1 ± 8.8‡‡ ¶	54.4 ± 8.0	60.3 ± 8.7	0.0326

HR, heart rate ; SBP, systolic blood pressure ; DBP, diastolic blood pressue ; BNP, brain natriuretic peptide ; LAD, left atrial diameter ; LVEDD, left ventricular end diastolic diameter ; LVESD, left ventricular end systolic diameter ; FS, fractional shortening ; IVS, interventircular septum ; Thd, thickness at end-diastole ; PW, posterior wall ; EF, ejection fraction ; *, P < 0.0001 vs. normal ; †, P < 0.0001 vs. group 1 ; ‡, P < 0.0001 vs. group 2 ; §, P < 0.001 vs. normal ; **, P < 0.001 vs. group 1 ; ††, P < 0.001 vs. group 2 ; ‡‡, P < 0.05 vs. normal ; §§, P < 0.05 vs. group 1 ; ¶, P < 0.05 vs. group 2

Table 2　Doppler flow parameters (Mean ± SD)

Variable	Normal	Group 1 (No LVH)				Group 2 (LVH)				Group 3 (CHF)			
	(n = 20)	Overall (n = 32)	AL (n = 22)	ATTRm (n = 10)	P value	Overall (n = 23)	AL (n = 9)	ATTRm (n = 14)	P value	Overall (n = 43)	AL (n = 16)	ATTRm (n = 27)	P value
TMF-E/A	1.03 ± 0.24	1.00 ± 0.27	0.94 ± 0.18	1.16 ± 0.39	0.0174	0.94 ± 0.62	0.82 ± 0.22	1.00 ± 0.77	0.733	1.27 ± 0.78	1.28 ± 0.90	1.27 ± 0.72	0.636
TMF-E-DT (ms)	200 ± 53	218 ± 51	216 ± 49	225 ± 59	0.887	279 ± 69[‖]	240 ± 65	304 ± 62	0.041	224 ± 71[#]	194 ± 51	242 ± 76	0.036
IVRT (ms)	106 ± 21	102 ± 18	106 ± 19	93 ± 12	0.08	122 ± 42	116 ± 39	126 ± 45	0.393	108 ± 33	92 ± 33	117 ± 31	0.0261
PEP (ms)	82 ± 14	77 ± 13	76 ± 12	80 ± 14	0.511	88 ± 21	85 ± 14	89 ± 24	0.613	92 ± 28[**]	73 ± 11	103 ± 29	0.0009
ET (ms)	305 ± 24	322 ± 30	330 ± 26	305 ± 32	0.076	292 ± 48[**]	273 ± 55	304 ± 40	0.095	297 ± 38[**]	276 ± 47	309 ± 27	0.002
PVF-D/S	0.77 ± 0.21	0.84 ± 0.24	0.76 ± 0.14	1.01 ± 0.32	0.0124	0.88 ± 0.83	0.71 ± 0.16	0.98 ± 1.06	0.729	1.29 ± 0.86[*††]	1.29 ± 0.97	1.30 ± 0.80	0.773
E/e' (septum)	8.9 ± 1.6	10.1 ± 3.3	9.5 ± 2.9	11.3 ± 4.0	0.247	15.5 ± 7.5	13.6 ± 6.7	16.8 ± 8.0	0.270	22.0 ± 11.5[*†††‡‡]	19.0 ± 12.5	23.8 ± 10.6	0.027
E/e' (lateral)	7.4 ± 2.8	7.7 ± 2.2	7.5 ± 2.0	8.0 ± 2.8	0.855	10.6 ± 4.6	10.2 ± 4.1	10.9 ± 5.0	0.900	16.1 ± 8.1[*†]	15.2 ± 7.3	16.6 ± 8.7	0.624

TMF, transmitral flow ; E/A, early to late velocity ratio of mitral inflow ; TMF-E-DT, deceleration time of transmitral E flow ; IVRT, isovolumic relaxation time ; PEP, pre ejection period ; ET, ejection time ; PVF, pulmonary venous flow ; PVF-D/S, pulmonary venous flow D/S velocity ratio ; E/e', mitral inflow to mitral relaxation velocity ratio ; [*], P < 0.0001 vs. normal ; [†], P < 0.0001 vs. group 1 ; [‡], P < 0.0001 vs. group 2 ; [§], P < 0.01 vs. normal ; [‖], P < 0.01 vs. group 1 ; [#], P < 0.01 vs. group 2 ; [**], P < 0.05 vs. normal ; [††], P < 0.05 vs. group 1 ; [‡‡], P < 0.05 vs. group 2

Table 3　Global left ventricular strain values

Variable	Normal	Group 1 (No LVH)				Group 2 (LVH)				Group 3 (CHF)			
	(n = 20)	Overall (n = 32)	AL (n = 22)	ATTRm (n = 10)	P value	Overall (n = 23)	AL (n = 9)	ATTRm (n = 14)	P value	Overall (n = 43)	AL (n = 16)	ATTRm (n = 27)	P value
Basal GCS (inner)	−19.9 ± 3.0	−20.7 ± 3.9	−20.3 ± 3.4	−21.6 ± 4.8	0.699	−18.3 ± 4.1	−17.3 ± 4.4	−18.9 ± 3.9	0.431	−18.8 ± 4.4	−17.8 ± 4.5	−19.4 ± 4.3	0.253
Basal GCS (outer)	−12.3 ± 2.0	−13.1 ± 2.9	−13.1 ± 2.6	−13.2 ± 3.6	1.0	−11.1 ± 3.1	−10.4 ± 2.7	−11.5 ± 3.3	0.270	−11.7 ± 3.4	−11.0 ± 3.8	−12.0 ± 3.2	0.191
Mid GCS (inner)	−19.2 ± 3.0	−20.0 ± 4.3	−20.1 ± 4.1	−19.8 ± 5.1	0.951	−18.9 ± 3.9	−18.3 ± 5.0	−19.2 ± 3.1	0.561	−18.8 ± 4.4	−17.2 ± 4.8	−19.7 ± 4.0	0.105
Mid GCS (outer)	−11.6 ± 1.8	−12.2 ± 2.7	−12.1 ± 2.5	−12.5 ± 3.2	0.823	−12.3 ± 2.8	−11.4 ± 3.5	−11.2 ± 2.5	0.682	−11.6 ± 3.3	−10.2 ± 3.8	−12.4 ± 2.8	0.0578
Basal GRS (inner)	25.8 ± 6.0	19.7 ± 6.1**	19.4 ± 5.6	20.2 ± 7.4	0.730	14.1 ± 9.5*‡‡	15.4 ± 12.1	13.2 ± 7.8	0.875	10.6 ± 6.9*†	10.5 ± 5.6	10.7 ± 7.6	0.811
Basal GRS (outer)	21.3 ± 5.9	21.9 ± 5.7	20.7 ± 5.3	24.7 ± 5.8	0.077	16.1 ± 6.1|	15.7 ± 7.7	16.3 ± 5.1	0.925	15.8 ± 7.9‖**	13.5 ± 6.7	17.1 ± 8.3	0.189
Mid GRS (inner)	22.6 ± 6.5	20.8 ± 5.8	20.3 ± 4.6	21.9 ± 8.0	0.951	16.3 ± 7.2|	16.5 ± 9.0	16.1 ± 6.2	0.777	14.2 ± 7.5§|	14.2 ± 6.6	14.2 ± 8.1	0.811
Mid GRS (outer)	18.9 ± 6.3	19.5 ± 7.3	19.1 ± 6.9	20.3 ± 8.5	0.984	18.7 ± 6.7	20.6 ± 8.4	17.5 ± 5.3	0.469	18.0 ± 7.7	16.7 ± 6.5	18.9 ± 8.4	0.6660
Global LS 4CH													
Global LS (inner)	−15.4 ± 1.9	−15.4 ± 2.3	−15.4 ± 2.3	−15.5 ± 2.4	0.340	−11.5 ± 2.9§†	−11.5 ± 2.4	−11.5 ± 3.2	0.856	−10.6 ± 3.4*†	−11.2 ± 3.6	−10.3 ± 3.3	0.506
Global LS (outer)	−13.8 ± 2.2	−13.0 ± 1.9	−13.1 ± 2.1	−12.8 ± 1.4	0.371	−9.9 ± 2.1*	−9.6 ± 1.6	−10.0 ± 2.4	0.638	−8.6 ± 3.4*	−9.3 ± 3.2	−8.2 ± 3.6	0.223
Global LS 2CH													
Global LS (inner)	−16.0 ± 2.4	−15.8 ± 2.4	−15.8 ± 2.2	−15.6 ± 2.8	0.405	−12.7 ± 3.4††	−11.8 ± 2.3	−13.2 ± 3.9	0.180	−12.4 ± 5.4**‖	−14.4 ± 7.6	−11.4 ± 3.4	0.149
Global LS (outer)	−14.8 ± 2.5	−13.1 ± 2.4	−13.4 ± 2.7	−12.7 ± 1.3	0.215	−10.8 ± 2.6*††	−10.2 ± 2.1	−11.2 ± 2.8	0.328	−9.5 ± 3.1*†	−10.1 ± 3.4	−9.1 ± 2.9	0.205
Global LS ALAX													
Global LS (inner)	−15.7 ± 3/4	−15.4 ± 2.3	−15.4 ± 2.3	−15.5 ± 2.4	0.971	−11.5 ± 2.9|**	−11.5 ± 2.4	−11.5 ± 3.2	0.856	−10.6 ± 3.4†**	−11.2 ± 3.6	−10.3 ± 3.3	0.506
Global LS (outer)	−13.1 ± 2.9	−13.0 ± 1.9	−13.1 ± 2.1	−12.8 ± 1.4	0.371	−9.9 ± 2.1§‖	−9.6 ± 1.6	−10.0 ± 2.4	0.638	−8.6 ± 3.4*†	−9.3 ± 3.2	−8.2 ± 3.6	0.223

ALAX, apical long axis view ; 4CH, 4-chamber view ; 2CH, 2-chamber view ; GCS, global circumferential strain ; GRS, global radial strain ; LS, longitudinal strain ; *, P < 0.0001 vs. normal ; †, P < 0.0001 vs. group 1 ; ‡, P < 0.0001 vs. group 2 ; §, P < 0.01 vs. normal ; |, P < 0.01 vs. group 1 ; #, P < 0.01 vs. group 2 ; **, P < 0.05 vs. normal ; ††, P < 0.05 vs. group 1 ; ‡‡, P < 0.05 vs. group 2

but there was no difference in outer global radial strain among the three groups. Global longitudinal strains in all apical 3 views were smaller in groups 2 and 3 than in group 1 and controls for both the inner and outer myocardial layers. No strain echo parameter showed differences between those with AL and ATTRm amyloidoses.

Segmental strain measurements are shown in **Fig. 1–3**. Representative strain analyses are shown in **Fig. 1** and **Fig. 2**, **Fig. 1** shows the circumferential strain, **Fig. 2** shows the radial strain in a patient of group 1and group 3. Circumferential strain of the inner layer was greater than that of the outer layer in a patient of group 1 and group 3. **(Fig. 1A, B) Fig. 2A** shows a greater value for the inner radial strain compared to that of the outer layer, but radial strain of the inner layer was smaller than that of the outer layer **(Fig. 2B)**.

In the base and mid-LV wall, most segmental circumferential strain was not significantly different among three groups in both layers **(Fig. 3A)**. Regarding segmental radial strain, many segments in group 3 showed a lower radial strain compared to that of group 1. Inner radial strains were greater in normal individuals than in the other 3 groups in many myocardial segments as shown in **Fig. 3B**. Basal and mid-radial radial strain of the outer layer did not differ among the 4 groups in most segments. Longitudinal segmental strain values are shown in **Fig. 3C**. Most basal and mid-longitudinal strain values were smaller in groups 2 and 3 than in group 1 for both the inner and outer myocardial layers, and those in normal individuals showed greater values than in the other 3 groups.

E Reproducibility of strain measurements

Reproducibility of the measurements is summarized in **Table 4**. The intraobserver and interobserver agreement for the segmental longitudinal, circumferential, and radial strain of the inner and outer myocardial layers was excellent; the coefficients of variation for the intraobserver and interobserver comparison were＜5 %.

Ⅳ Discussion

To the best of our knowledge, this was the first study to demonstrate endomyocardial dysfunction in patients with CA using speckle tracking echocardiography. In patients with advanced CA, complete endomyocardial radial systolic dysfunction existed predominantly in the basal and mid-LV wall; and longitudinal transmural LV systolic dysfunction existed predominantly in the basal and mid-LV wall with apical sparing. However, there were no significant differences in circumferential inner/outer strain among three groups in the basal and mid-LV wall.

Previous studies have demonstrated that CMRI shows a distinct pattern of late gadolinium enhancement, which is distributed over the entire subendocardial circumference, extending in various degrees into the neighboring myocardium. This pattern is specific for CA[24)30)31)]. Our study demonstrated complete subendocardial radial dysfunction in patients with cardiac involvement, which is very similar to the CMRI pattern of late gadolinium enhancement. The mechanism of the specific pattern of LV longitudinal and radial dysfunction (i.e., inner layer dominant myocardial dysfunction) and preserved circumferential strain may be explained by the amyloid deposition pattern in CA as follows. In the LV inner (endocardial) layer, longitudinally oriented myocardial fibers exist, which contribute to LV longitudinal and inner LV layer radial function. The specific pattern of amyloid deposition in the endocardial layer may cause longitudinal systolic dysfunction, which can lead to worse longitudinal and radial (i.e., inner layer dominant) LV strain. However, LV circumferential myocardial fiber exists in the mid and outer layers of the LV myocardium. Consequently, circumferential LV shortening (i.e., strain) may be preserved until amyloid infiltration progresses to the mid- to outer layers in advanced cardiac amyloidosis.

We also demonstrated that a multidirectional strain pattern is not different between AL and ATTRm cardiac amyloidosis.

This study clarified that inner radial strain was smaller in group 1 than in normal controls. Fifty of

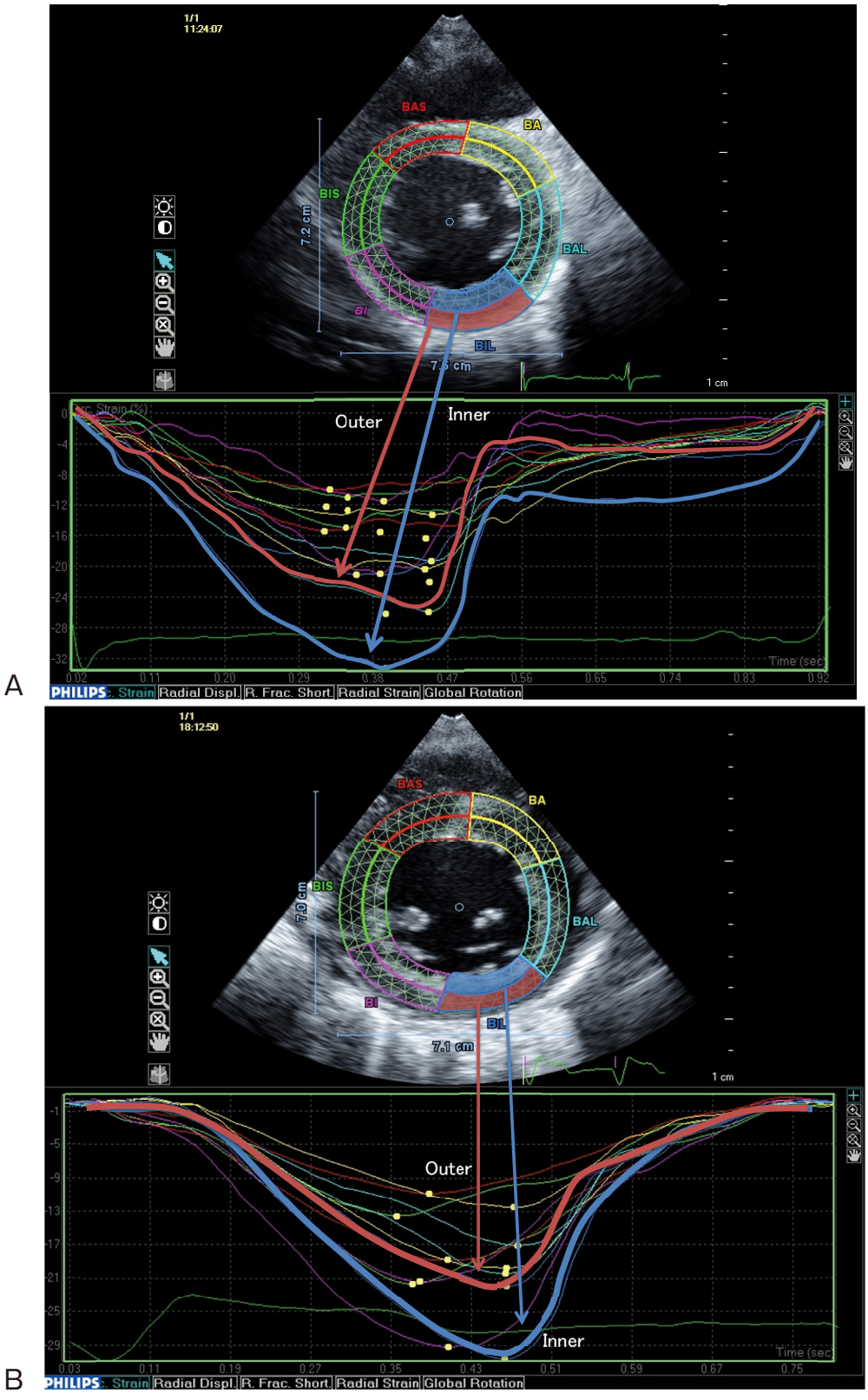

Fig. 1

A : Segmental circumferential strain of a patient in group 1. The absolute value of circumferential strain in the inner layer (blue line) is greater than that in the outer layer (orange line).

B : Segmental circumferential strain of a patient in group 3. The absolute value of circumferential strain in the inner layer (blue line) is greater than that in the outer layer (orange line), which is similar to that of the patient in group 1.

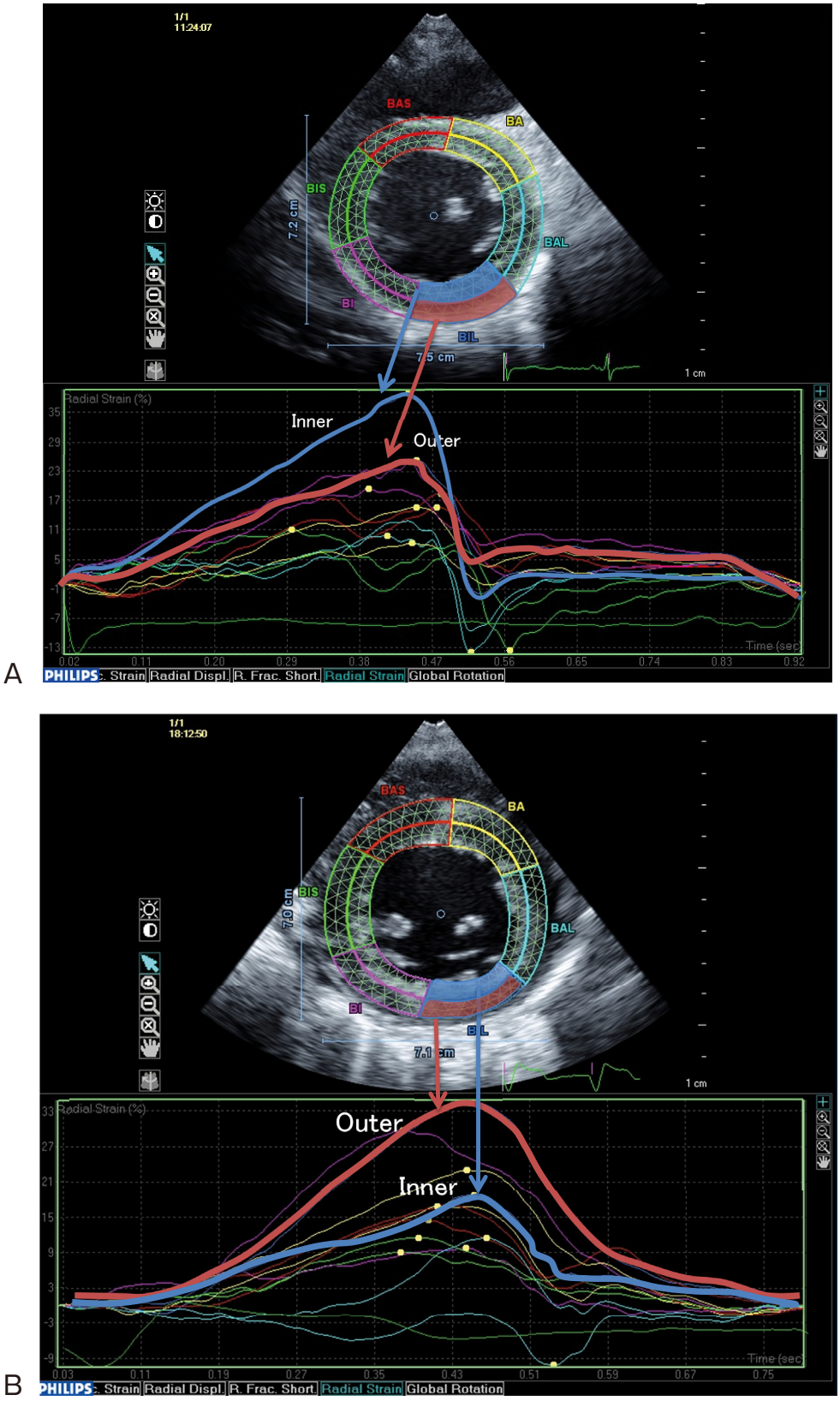

Fig. 2

A : Segmental radial strain of a patient in group 1. Segmental inner radial strain (blue line) is greater than that in the outer layer (orange line)

B : Segmental radial strain of a patient in group 3. Segmental radial strain of the inner layer (blue line) is smaller than that of the outer layer (orange line) in advanced cardiac amyloidosis.

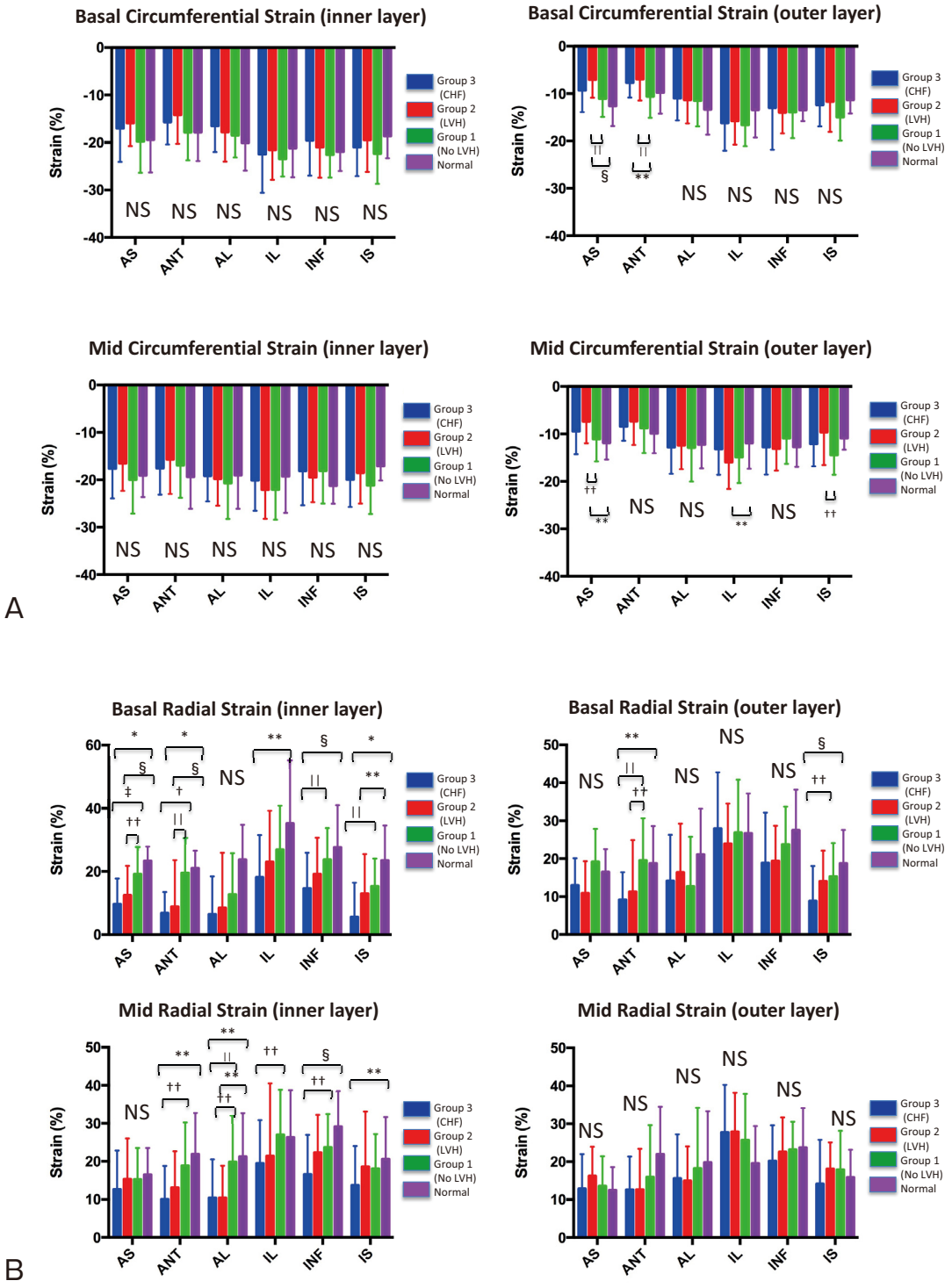

Fig. 3

A : Segmental circumferential strain of the inner and outer layers in the basal and mid left ventricle. Most of the segmental circumferential strain is not significantly different among three groups in both layers, except for several segments. AL, antero-lateral ; ANT, anterior ; AS, antero-septum ; IL, infero-lateral ; INF, inferior ; IS, infero-septum ; §, P<0.01 vs. normal ; ‖, P<0.01 vs. group 1 ; **, P<0.05 vs. normal ; ††, P<0.05 vs. group 1.

B : Segmental radial strain of the inner and outer layers in the basal and mid left ventricle. AL, antero-lateral ; ANT, anterior ; AS, antero-septum ; IL, infero-lateral ; INF, inferior ; IS, infero-septum ; *, P<0.0001 vs. normal ; †, P<0.0001 vs. group 1 ; ‡, P<0.0001 vs. group 2 ; §, P<0.01 vs. normal ; ‖, P<0.01 vs. group 1 ; #, P<0.01 vs. group 2 ; **, P<0.05 vs. normal ; ††, P<0.05 vs. group 1 ; ‡‡, P<0.05 vs. group 2.

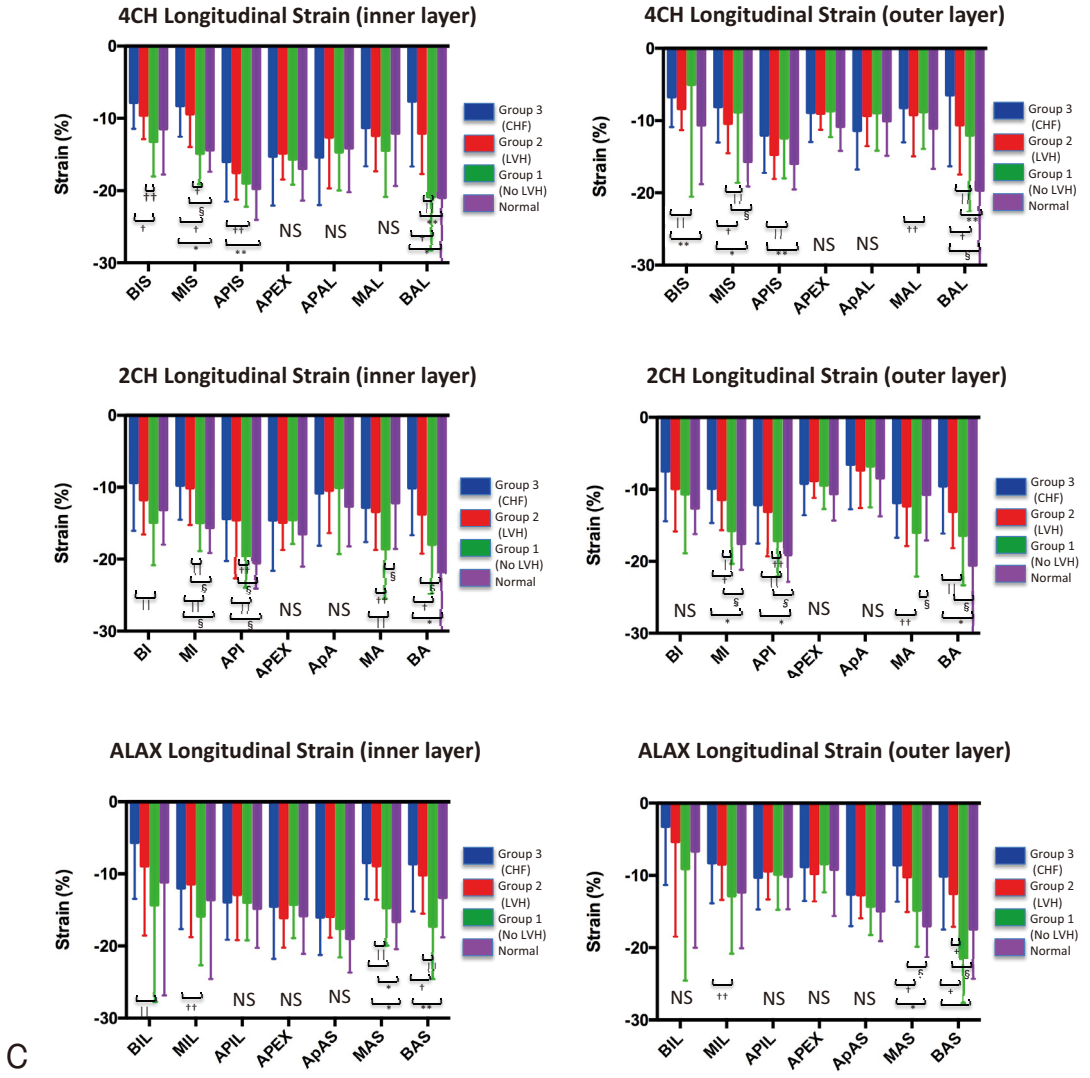

C

Fig. 3

C : Segmental longitudinal strain of the inner and outer layers in apical four-, two-, and long axis views. Most basal and mid-longitudinal strain values are smaller in groups 2 and 3 compared to those in group 1 in both the inner and outer myocardial layers.

4CH, apical four chamber view ; 2CH, apical two chamber view ; ALAX , apical long axis view ; ApA, apical anterior ; APAL, apical antero-lateral ; ApAS, apical antero-septum ; API, apical inferior ; APIL, apical infero-lateral ; APIS, apical inter-ventricular septum ; BA, basal anterior ; BAL, basal antero-lateral ; BAS, basal antero-septum ; BI, basal inferior ; BIL, basal infero-lateral ; BIS, basal inter-ventricular septum ; MA, mid anterior ; MAL, mid antero-lateral ; MAS, mid antero-septum ; MI, mid inferior ; MIL, mid infero-lateral ; MIS, mid inter-ventricular septum ; *, $P<0.0001$ vs. normal ; †, $P<0.0001$ vs. group 1 ; ‡, $P<0.0001$ vs. group 2 ; §, $P<0.01$ vs. normal ; ‖, $P<0.01$ vs. normal ; **, $P<0.05$ vs. normal ; ††, $P<0.05$ vs. group

Table 4 Reproducibility of measurements

	Intraobserver agreement (mean ± 1.96 SD) (%)	Coefficient variation for intraobserver comparisons (%)	Interobserver agreement (mean ± 1.96 SD) (%)	Coefficient variation for interobserver comparisons (%)
Longitudinal strain				
Inner	0.10 ± 0.55	2.1	0.02 ± 0.55	2.1
Outer	− 0.01 ± 0.47	2.2	0.02 ± 0.51	2.4
Circumferential strain				
Inner	− 0.04 ± 0.81	2.1	− 0.05 ± 0.43	2.1
Outer	− 0.13 ± 0.99	4.1	− 0.03 ± 0.63	2.5
Radial strain				
Inner	0.05 ± 0.92	3.2	0.01 ± 0.65	2.2
Outer	− 0.05 ± 0.97	2.7	0.03 ± 0.83	2.3

SD, standard deviation

51 patients with ATTRm showed a positive shadow on myocardial ^{99m}Tc pyrophosphate scintigraphy in our study. This finding suggested that myocardial amyloid deposition exists even in patients with normal LV thickness. In AL amyloidosis, it is also reported that impaired LV systolic function by Doppler myocardial imaging exists in patients with AL amyloidosis and no evidence of cardiac involvement by standard 2-dimensional and Doppler echocardiography and this report is consistent with our results[32].

A Limitations

CA was defined as a mean value of LV thickness >12 mm in patients with CA confirmed by a biopsy from any site, thus many patients were diagnosed with CA without an endomyocardial biopsy. However, based on autopsy studies, an echocardiographic finding of LV thickening in the absence of diseases associated with LV hypertrophy is generally accepted as highly specific for the finding of CA at biopsy or autopsy[33]. No other cardiac imaging such as cardiac magnetic resonance imaging for the quantification of myocardial amyloid deposition was included in this study. Because some patients with CA already had renal dysfunction, we could not perform gadolinium enhancement.

Conclusions

A multi-layer approach of measuring myocardial strain demonstrated complete endomyocardial radial systolic dysfunction and longitudinal transmural systolic dysfunction with apical sparing in patients with CA.

References

1) Falk RH, Comenzo RL, Skinner M : The systemic amyloidoses. N Engl J Med 337 : 898-909, 1997
2) Falk RH : Diagnosis and management of the cardiac amyloidosis. Circulation 112 : 2047-2060, 2005
3) Falk RH : Cardiac amyloidosis : a treatable disease, often overlooked. Circulation 124 : 1079-1085, 2011
4) Swanton RH, Brooksby IA, Davies MJ, Coltart DJ, Jenkins BS, Webb-Peploe MM : Systolic and diastolic ventricular function in cardiac amyloidosis. Studies in six cases diagnosed with endomyocardial biopsy. Am J Cardiol 39 : 658-664, 1997
5) Ruberg FL, Berk JL : Transthyretin (TTR) cardiac amyloidosis. Circulation 126 : 1286-1300, 2012
6) Siqueira-Filho AG, Cunha CL, Tajik AJ, Seward JB, Schattenberg TT, Giuliani ER : M-mode and two-dimensional echocardiographic features in cardiac amyloidosis. Circulation 63 : 188-196, 1981
7) St John Sutton MG, Reichek N, Kastor JA, Giuliani ER : Computerized M-mode echocardiographic analysis of left ventricular dysfunction in cardiac amyloid. Circulation 66 : 790-799, 1982
8) Roberts WC, Waller BF : Cardiac amyloidosis causing cardiac dysfunction : analysis of 54 necropsy patients. Am J

Cardiol 52 : 137–146, 1983

9) Cueto-Garcia L, Reeder GS, Kyle RA, Wood DL, Seward JB, Naessens J, Offord KP, Greipp PR, Edwards WD, Tajik AJ : Echocardiographic findings in systemic amyloidosis : spectrum of cardiac involvement and relation to survival. J Am Coll Cardiol 6 : 737–743, 1985

10) Falk RH, Plehn JF, Deering T, Schick EC Jr., Boinay P, Rubinow A : Sensitivity and specificity of the echocardiographic features of cardiac amyloidosis. Am J Cardiol 59 : 418–422, 1987

11) Klein AL, Hatle LK, Burstow DJ, Seward JB, Kyle RA, Bailey KR, Luscher TF, Gertz MA, Tajik AJ : Doppler characterization of left ventricular diastolic function in cardiac amyloidosis. J Am Coll Cardiol 13 : 1017–1026, 1989

12) Klein AL, Hatle LK, Taliercio CP, Taylod CL, Kyle RA, Bailey KR, Seward JB, Tajik AJ : Serial Doppler echocardiographic follow-up of left ventricular diastolic function in cardiac amyloidosis. J Am Coll Cardiol 16 : 1135–1141, 1990

13) Klein AL, Hatle LK, Taliercio CP, Oh JK, Kyle RA, Gertz MA, Bailey KR, Seward JB, Tajik AJ : Prognostic significance of Doppler measures of diastolic function in cardiac amyloidosis. Circulation 83 : 808–816, 1991

14) Tei C, Dujardin KS, Hodge DO, Kyle RA, Tajik AJ, Seward JB : Doppler index combining systolic and diastolic myocardial performance : clinical value in cardiac amyloidosis. J Am Coll Cardiol 28 : 658–664, 1996

15) Koyama J, Ray-Sequin PA, Falk RH : Longitudinal myocardial function assessed by tissue velocity, strain, and strain rate tissue Doppler echocardiography in patients with AL (primary) cardiac amyloidosis. Circulation 107 : 2446–2452, 2003

16) Koyama J, Falk RH : Prognostic significance of strain Doppler imaging in light-chain amyloidosis. JACC Cardiovasc Imaging 3 : 333–342, 2010

17) Bellavia D, Pellikka PA, Al-Zahrani GB, Abraham TP, Dispenzieri A, Miyazaki C, Lacy M, Scott CG, Oh JK, Miller FA Jr. : Independent predictors of survival in primary systemic (Al) amyloidosis, including cardiac biomarkers and left ventricular strain imaging : an observational cohort study. J Am Soc Echocardiogr 23 : 643–652, 2010

18) Buss SJ, Emami M, Mereles D, Korosoglow G, Kristen AV, Voss A, Schellberg D, Zugck C, Galuschky C, Giannitsis E, Hegenbart U, Ho AD, Katus HA, Schonland SO, Hardt SE : Longitudinal left ventricular function for prediction of survival in systemic light-chain amyloidosis : incremental value compared with clinical biochemical markers. J Am Coll Cardiol 60 : 1067–1076, 2012

19) Liu D, Hu K, Niemann M, Herrmann S, Cikes M, Stork S, Beer M, Gaudron PD, Morbach C, Knop S, Geissinger E, Ertl G, Bijnens B, Weidemann F : Impact of regional left ventricular function on outcome for patients with AL amyloidosis. PLoS One 8 : e56923, 2013

20) Quarta CC, Solomon SD, Uraizee I, Kruger J, Longhi S, Ferlito M, Gagliardi C, Milandri A, Rapezzi C, Falk RH : Left ventricular structure and function in transthyretin-related versus light-chain cardiac amyloidosis. Circulation 129 : 1840–1849, 2014

21) Koyama J, Ikeda S, Ikeda U : Echocardiographic assessment of the cardiac amyloidoses. Circ J 79 : 721–734, 2015

22) Maceira AM, Joshi J, Prasad SK, Moon JC, Perugini E, Harding I, Sheppard MN, Poole-Wilson PA, Hawkins PN, Pennell DJ : Cardiovascular magnetic resonance in cardiac amyloidosis. Circulation 111 : 186–193, 2005

23) Perugini E, Rapezzi C, Piva T, Leone O, Bacchi-Reggiani L, Riva L, Salvi F, Lovato L, Branzi A, Fattori R : Non-invasive evaluation of the myocardial substrate of cardiac amyloidosis by gadolinium cardiac magnetic resonance. Heart 92 : 343–349, 2006

24) Vogelsberg H, Mahrholdt H, Deluigi CC, Yilmaz A, Kispert EM, Greulich S, Klingel K, Kandolf R, Sechtem U : Cardiovascular magnetic resonance in clinically suspected cardiac amyloidosis : noninvasive imaging compared to endomyocardial biopsy. J Am Coll Cardiol 51 : 1022–1030 , 2008

25) Zhang Q, Fang F, Liang Y-J, Xie J-M, Wen Y-Y, Yip G W-K, Lam YY, Chan JY, Fung JW, Yu CM : A novel multi-layer approach of measuring myocardial strain and torsion by 2 D speckle tracking imaging in normal subjects and patients with heart diseases. Int J Cardiol 147 : 32–37, 2011

26) Ikeda S, Nakano T, Yanagisawa N, Nakazato M, Tsukagoshi H : Asymptomatic homozygous gene carrier in a family with type I familial amyloid polyneuropathy. Eur Neurol 32 : 308–313, 1992

27) Tachibana N, Tokuda T, Yoshida K, Taketomi T, Nakazato M, Li YF, Masuda Y, Ikeda S : Usefulness of MALDI/TOF mass spectrometry of immunoprecipitated serum variant transthyretin in the diagnosis of familial amyloid polyneuropathy. Amyloid 6 : 282–288, 1999

28) Schiller NB, Shah PM, Crawford M, DeMaria A, Devereux R, Feigenbaum H, Gutgesell H, Reichek N, Sahn D, Schnittger I : Recommendations for quantitation of the left ventricle by two-dimensional echocardiography. American Society of Echocardiography Committee on Standards, Subcommittee on Quantitation of Two-Dimensional Echocardiograms. J Am Soc Echocardiogr 2 : 358–367, 1989

29) Lang RM, Bierig M, Devereux RB, Flachskampf FA, Foster E, Pellikka PA, Picard MH, Roman MJ, Seward J, Shanewise JS, Solomon SD, Spencer KT, Sutton MS, Stewart WJ ; Chamber Quantification Writing Group ; American Society of Echocardiography's Guidelines and Standards Committee ; European Association of Echocardiography. Recommendations for chamber quantification : a report from the American Society of Echocardiography's Guidelines and Standards Committee and the Chamber Quantification Writing Group, developed in conjunction with the European Association of Echocardiography, a branch of the European Society of Cardiology : J Am Soc Echocardiogr 18 : 1440–1463, 2005

30) Syed IS, Glockner JF, Feng D, Araoz PA, Martinez MW, Edwards WD, Gertz MA, Dispenzieri A, Oh JK, Bellavia D, Tajik AJ, Grogan M : Role of cardiac magnetic resonance imaging in the detection of cardiac amyloidosis. JACC Cardiovasc Imaging 3 : 155–164, 2010

31) Mongeon FP, Jerosch-Herold M, Coelho-Filho OR, Blankstein R, Falk RH, Kwong RY : Quantification of extracellular matrix expansion by CMR in infiltrative heart disease. JACC Cardiovasc Imaging 5 : 897–907, 2012

32) Bellavia D, Pellikka PA, Abraham TP, Al-Zahrani GB, Dispenzieri A, Oh JK, Bailey KR, Wood CM, Lacy MQ, Miyazaki C, Miller FA Jr. : Evidence of impaired left ventricular systolic function by Doppler myocardial imaging in patients with systemic amyloidosis and no evidence of cardiac involvement by standard two-dimensional and Doppler echocardiography. Am J Cardiol 101 : 1039–1045, 2008

33) Arbustini E, Verga L, Concardi M, Palladini G, Obici L, Merlni G : Electron and immuno-electron microscopy of abdominal fat identifies and characterizes amyloid fibrils in suspected cardiac amyloidosis. Amyloid 9 : 108–114, 2002

(2018. 8. 17 received ; 2018. 10. 11 accepted)